Digest Journal of Nanomaterials and Biostructures Vol. 6, No 4, October-December 2011, p. 1597-1603

SYNTHESIS AND CHARACTERIZATION OF Pb^+ DOPED MgO NANOCRYSTALLINE PARTICLES

S. SURESH*, D.ARIVUOLI
Crystal Growth Centre, Anna University, Chennai-600 025, India

Nanocrystalline particles of Pb^+ doped MgO were prepared by a low-temperature combustion method. The crystalline nature and particle size of the samples were characterized by Powder X-ray diffraction analysis (XRD). The morphology of prepared nanocrystals was studied by scanning electron microscope (SEM) and the presence of Pb^+ in the sample was confirmed by energy dispersive X- ray analysis (EDX). The presence of functional groups in the samples was analyzed using FT-IR analysis. The optical absorption of the synthesized samples was studied using UV absorption spectral analysis.The frequency dependent dielectric behavior of the synthesized nano materials was analyzed.

(Received September 2, 2011; accepted October 13, 2011)

Keywords: Nanocrystalline materials, Powder X-ray diffraction, Scanning electron microscopy, EDX, FTIR analysis, UV-analysis

1. Introduction

In recent years, metal and semiconductor nano particles received considerable attention as active components in a wide variety of basic research and technological applications due to their improved optical, electric and magnetic properties compared to their bulk counter-parts [1-3]. Magnesium oxide is an interesting basic oxide that has many applications in catalysis, adsorption and in the synthesis of refractory ceramics [4–7]. It is a unique solid because of its highly ionic character, simple stoichiometry and crystal structure, and it can be prepared in widely variable particle sizes and shapes [8]. It has been documented that the shape and size of nanocrystalline magnesium oxide particles endow them with high specific surface and reactivity, because of the high concentration of edge/corner sites and structural defects on their surface [9].

In the present work, Pb^+ doped magnesium Oxdie nanocrystalline particles were synthesized by low-temperature combustion method. The synthesized samples were subjected to characterizations such as Powder X-ray diffraction analysis, SEM, EDX, FTIR, optical absorption analysis and dielectric studies.

2. Experimental procedure

The annular (AR) quality of Magnesium Nitrate, Lead Nitrate and Glycine were dissolved in deionized water. The solution was stirred, filtered and heated for five hours in a heating mantle. Bright white fumes were evolved at the final stage of the preparation by evolution of gases and leaving the end residue of MgO.PbO nanopowder. This powder was further annealed at 700˚C and placed in a decigator to avoid moisture absorption, since MgO has high moisture absorbing property. The synthesized MgO nanoparticle is white in color which is confirmed from the reported literature [10]. The Pb^+ sample pale yellow in color, which implies the formation of

*Corresponding author: sureshsagadevan@yahoo.co.in

β.PbO nanomaterials within the system of MgO. The sample further to fine powder in mortar and their powder was subjected to further characterization.

3. Results and discussion

3.1 Powder X-ray diffraction Analysis

Powder X-ray diffraction pattern of the synthesized sample was recorded using Pan Analytical x-pert instrument by means of a slowly moving radiation detector with a scan speed of 2˚/min in the range of 10-80˚ where monochromatic wavelength of 1.54Å (CuKα) was used. The obtained spectrum for pure and Pb^{+} doped MgO are shown in Figs1 and 2. From the spectrum of the pure sample, the fundamental peaks due to the diffraction of Mgo on the plane (111), (2 0 0), and (2 2 0) were obtained for synthesized samples, which is in good agreement with the reported value [11]. In Pb^{+} doped MgO spectrum the PbO fundamental XRD peaks were incorporated with the pure MgO. These confirm the presence of dopant in the MgO nanomaterials. The assigned hkl values of Pb^{+} doped MgO and the pure MgO were listed in the table. The X-ray diffraction spectrum of synthesized pure MgO shows only single phase system. But in the case of Pb^{+} doped sample, the spectrum consists of incorporation of Pb^{+} diffraction peaks, which changes the single phase into multiphase system. Also X-ray diffraction offers an easiest and fastest method to determine the particle size of the nanomaterials using the Debye - Scherrer equation

$$S = \frac{K\lambda}{\beta \cos\theta} \tag{1}$$

where K is a constant equal to 0.89, β is the full width half maximum height of the diffraction peak at angle θ and λ is wavelength. Implementing this equation it is found that pure sample is having a minimum size of 52 nm and Pb^{+} doped sample is having a minimum size of 50 nm. From the size it is confirmed that the synthesized material possess nano dimensional particles.

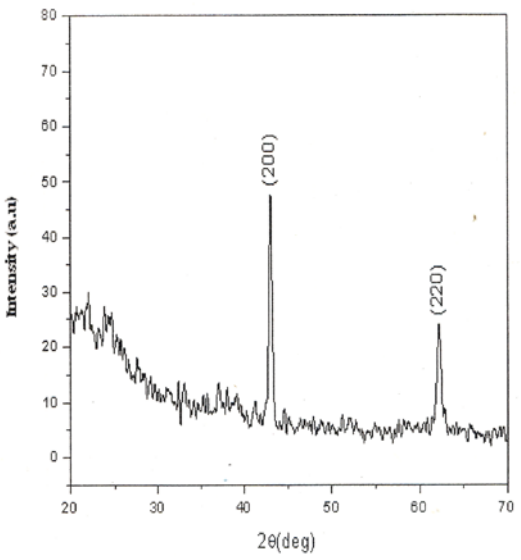

Fig.1 Powder XRD patterns of pure MgO

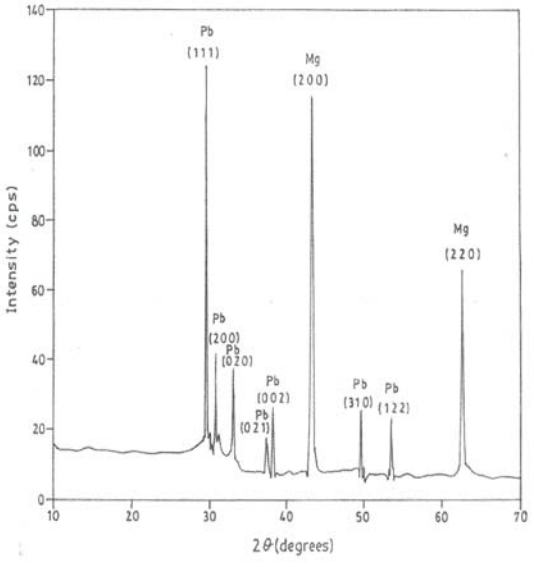

Fig.2 Powder XRD patterns of MgO and Pb^{+}

4. SEM analysis

The structure was analyzed by Scanning electron microscopy using JSM 840-A SEM. The obtained SEM images of MgO and MgO.Pb^{+} were shown in Figs 3 and 4. From the image it is observed that the synthesized sample of MgO has minimum particle size ranging between 40-50 nm. Also it shows that the materials possess porosity having pore diameter ranging from 10-50 nm. From the image of Pb^{+} doped sample, it was observed that the Pb^{+} crystalline nanoparticles was incorporated in the pores of the MgO compound with a minimum particle size ranging from 50-70 nm. Though the dopant was 5%, from the image it was found that Pb^{+} has mostly superimposed the MgO due to their higher molecular mass and atomic radii which was confirmed by EDX spectrum.

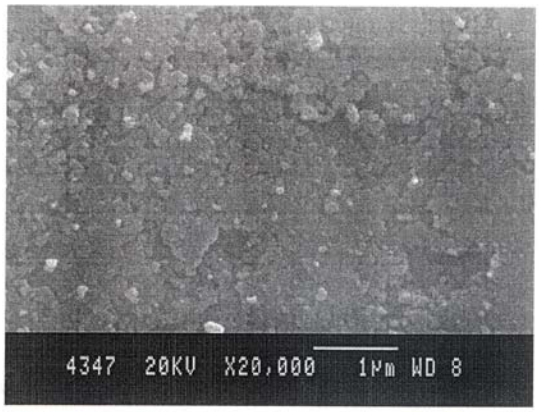

Fig.3 The SEM image of Pure MgO Nanocrystals

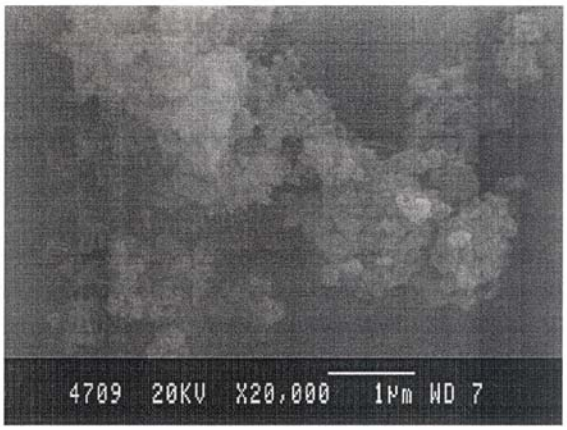

Fig.4 The SEM image of Pb^{+} Depoed MgO Nanocrystals

5. EDX analysis

The obtained EDX spectrums for both pure and doped samples are shown in Figs 5and6. From the pure sample spectrum 100% of Mg metal was observed in the sample corresponding to peak shown in the Fig.5. In doped sample the inclusion of Pb^{+} is shown in the corresponding peaks. From the data it is observed that the synthesized sample contains about Mg and Pb with 93.92 and 6.08% of atomic percentage respectively which agrees with expected value.

From the element count percentage, 64.44% of Mg and 35.56% of Pb have been observed. From these studies it was confirmed that, though Pb^{+} was 5% doped, it dominates the Mg metals due to their molecular mass, atomic radii and density. Also from the analysis, about 32% of cations are present in the 100% of sample.

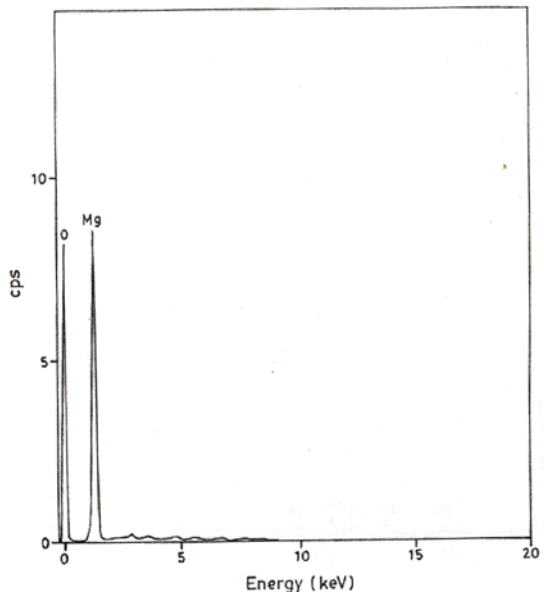

Fig.5 EDX spectrum of Pure MgO

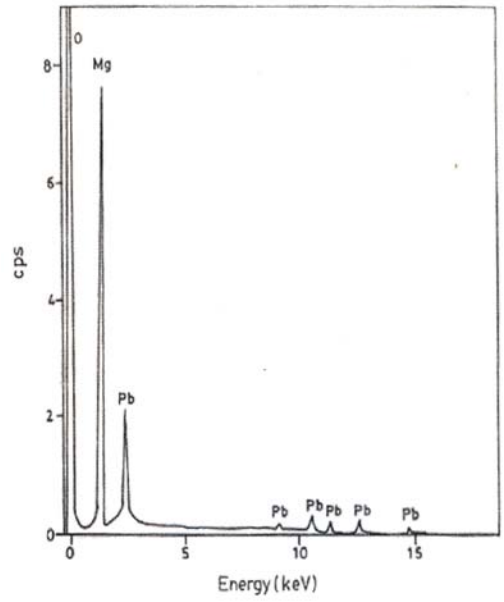

Fig.6 EDX spectrum of doped and MgO

6. FT-IR Analysis

The FTIR analysis of MgO and Pb^{+} doped MgO are shown in Figs 7 and 8. From the spectrum, the broadband 3500 to 2000 cm^{-1} is assigned to O-H bending vibration of the sample. This proves the moisture absorbing capacity of the sample. The frequencies of heteropolar diatomic molecules of MgO are confirmed by the peak at 863 cm^{-1}.

In the Pb^{+} doped MgO spectrum, overlapped peaks at 720cm^{-1} and 85 cm^{-1} confirm the vibrational frequencies of heteropolar diatomic molecular vibration of PbO and MgO respectively [12].

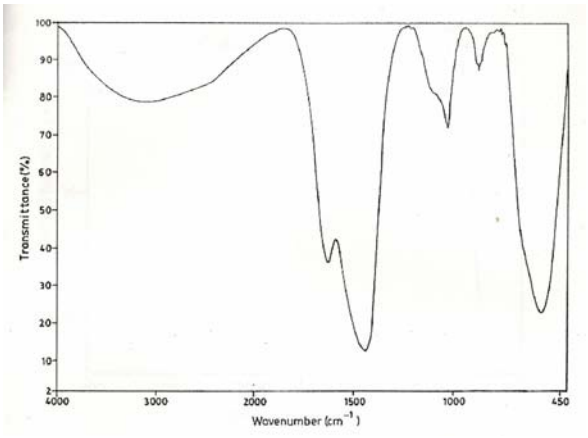

Fig.7 FTIR spectrum of Pure MgO

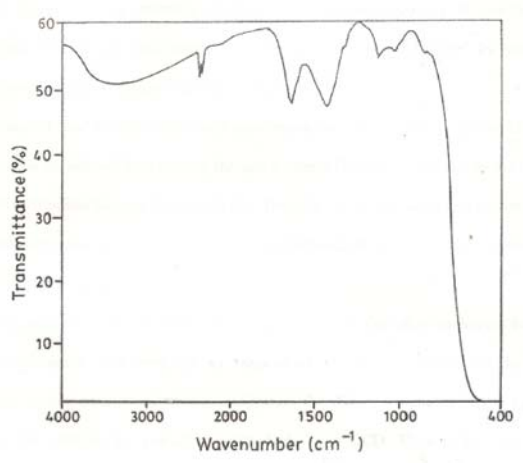

Fig.8 FTIR spectrum of doped and MgO

7. UV-Analysis

The UV absorption spectrum of MgO and Pb^{+} doped MgO samples are shown in Figs 9 and 10. From the spectrums it is observed that both the samples show very low absorption at entire IR and visible regions. This shows the optical transparency of the synthesized materials. For the pure MgO the UV cut off wavelength is found at 350 nm with sharp absorbance at the visible

region. Also the doped MgO shows shift in UV cut off wavelength at 420 nm. This is attributed due to incorporation of the dopant and shows broad absorption at UV region. So these materials can be used in ultraviolet region for the devices.

From the UV– absorption spectrum, the band gaps of the synthesized samples were calculated and both the samples shows direct band gap. The direct band gap materials obeys the following relation,

$$(\alpha h\nu)^2 = A(E_g - h\nu) \quad (2)$$

where α is absorption coefficient, E_g is the optical band gap of the material, A is a constant, h is Planck's constant and v is the frequency. The optical band gap of the samples has been calculated from the energy (h v) versus $(\alpha h\nu)^2$ plot shown in Fig 11. The band gap is found to be 2.9 and 3.5eV respectively and the variation in the band gap shows the presence of dopant in the synthesized material. Also the wide value of band gap reveals the large transmittance in the visible region than that in the UV -region [13].

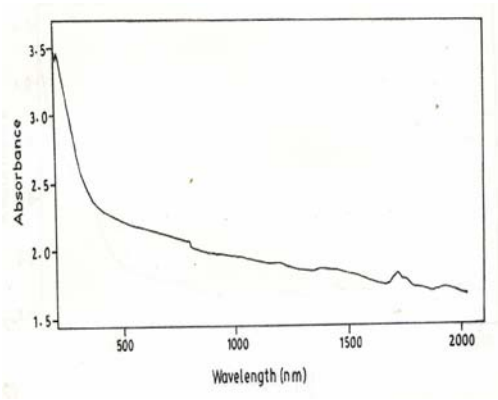

Fig.9 UV- spectrum of Pure MgO

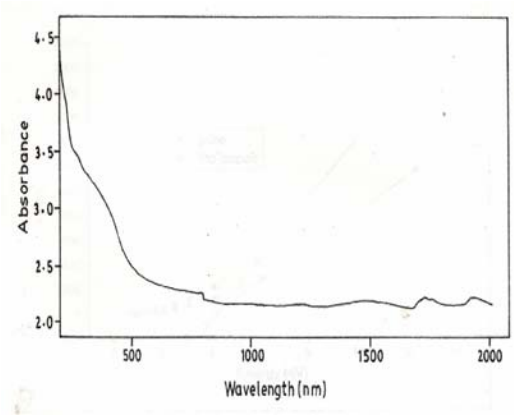

Fig.10 UV- spectrum of doped and MgO

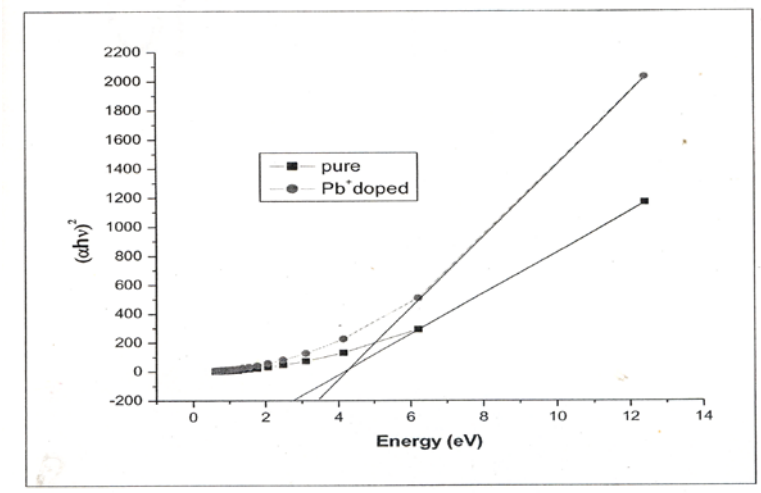

Fig.11 plot of photon energy (h v) vs $(\alpha h\nu)^2$

8. Dielectric Constant and Dielectric Loss

Dielectric constant and loss of the synthesized nanomaterials were calculated using HIOKI LCR Hitester 3532 in the frequency region 50 Hz to 5 MHz. The samples were pelletized and pellets of uniform dimension were placed between the two copper electrodes, which act as a parallel plate capacitor and silver paint was coated on the surface of the sample in order to make

firm ohmic contact. The capacitance and loss were measured for the applied frequency varying from 50 Hz to 5 MHz at different temperatures (40 ºC to 120 ºC).

A plot is drawn between log frequency and dielectric constant, the resulting plot was shown in Figs 12 and 13. From the plot it is observed that for both the samples the dielectric constant decreases with increase in frequency, which was in agreement with the reported value [11]. The dielectric constant of materials is due to the electronic, ionic, dipolar, and surface charge polarizations, which depend on the frequencies. The large value of dielectric constant at lower frequency may be due to space charge polarization arising at the grain boundary interfaces. The dielectric constant decreases with increase in temperature which is also in good agreement with the reported value. This was attributed due to space charge polarization. The plot of dielectric loss versus log frequency for both the samples is shown in Figs 14 and 15. From the plot, the dielectric loss also decreases with increase in frequency. The low dielectric loss confirms the purity of the synthesized sample.

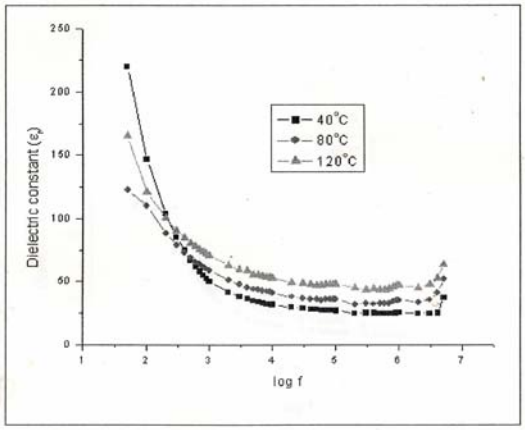

Fig.12 dielectric constant vs log f pure MgO

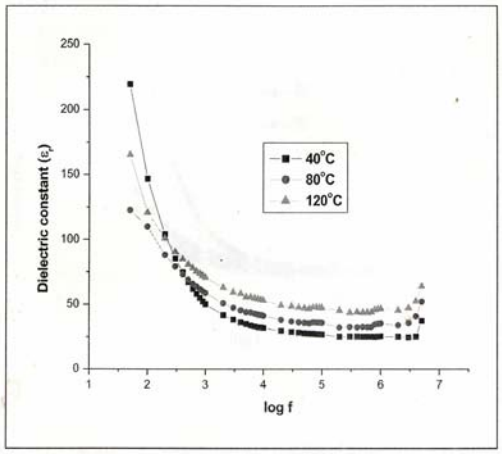

Fig.13 dielectric constant vs log f doped MgO

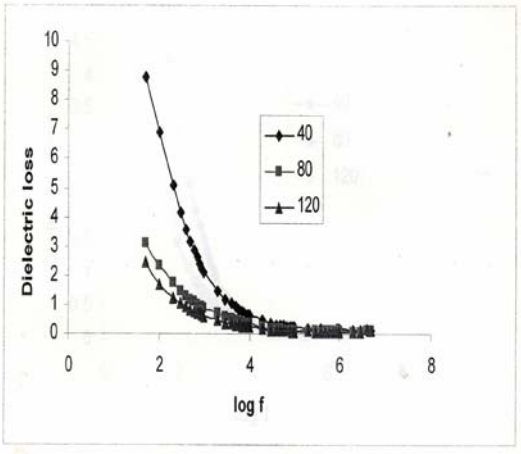

Fig.14 dielectric loss vs log f for pure MgO

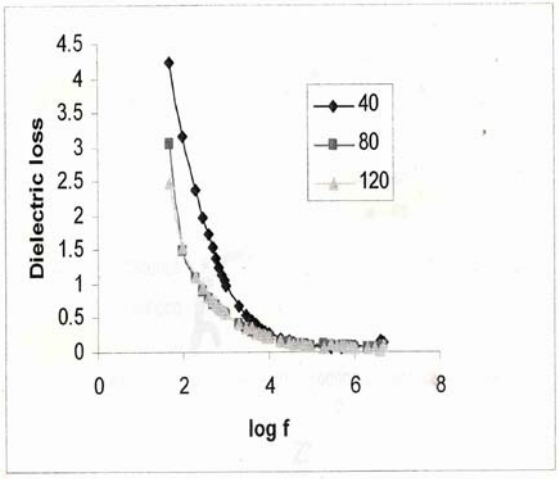

Fig.15 dielectric loss vs log f for doped MgO

9. Conclusion

Nanocrystalline particles of Pb^{+} doped MgO were synthesized by low-temperature combustion method. The Powder X- ray analysis confirmed the nanoparticle size and the fundamental diffraction patterns of MgO. The scanning electron microscopy and EDX analysis reveals the structure, morphology and inclusion of the dopants in the synthesized samples. FTIR spectrum for the synthesized samples, were recorded and the vibrations of the synthesized samples were studied. Optical property was studied by UV absorption spectrum of the samples, and high value of band gap reveals large transmittance in visible region than that in UV region reveals the

application towards optoelectronic devices. The frequency dependence of the dielectric constant and dielectric loss for the materials confirms the space charge polarization of the samples.

References

[1] V. F. Punfes, K. M. Krishnan, and A. P. Alivisatos, Science **291**, 245 (2001).
[2] Y. Xia, P. Yang, Y. Sun, B. Gate, Y. Yin, F. Kim, and H. Yan. Adv. Mater. **15**, 353 (2003).
[3] C. Salzemann, L. Lisieki, A. Brioude, J. Urban, and M. P. Pileni, J. Phys. Chem. B **108**, 13243 (2004).
[4] V.R.Choudhary, V.H.Rane, and R.V.Gadre, J. Catal., **145**, 300 (1994).
[5] S.Rajagopalan, S.Koper, S.Decker, J.Klabundek, Chem.Eur.**J8**, 2602(2002).
[6] B.Q.Xu, J.H.Wei, H.Y.Wang, K.Q.Sun, Q.M.Zhu, Cat.Today, **68**, 217(2001).
[7] S.Utampanya, K.J.Keabunde, J.R.Schlup, Chem.Mater. **3**,175(1991).
[8] R.M.Morris, K.J.Klabunde, Inorg.Chem. **22**, 682 (1983).
[9] K.J. Klabunde, J.Stark, O.Koper, C.Mohs, D.G.Park, S.Decker, Y.Jiang, I.Lagadic, D.Zhang. J.Phys.Chem. **100**, 12142 (1996).
[10] B.Nagappa, G.T.Chandrappa, Jacques Livage., Pramana Journal of Phys **65**, 917-923(2005).
[11] Xiao-Sheng Fang, Chang-Hui Ye, TingXie, Zhen-Yang Wong, Jian-Wei Zhao and Li-De Zhang, Applied Physics Letters, **88**, 013101 (2006).
[12] Kazuo Nakamoto, 3rd Edition, Wiley, New York, 1968.
[13] D.D.O.Eya, A.J.Ekpunobi, C.E.Okeke, Acadamic Open Internet Journal, **17,** (2006).